

Preliminary Cold Soaked Fuel Frost Studies with CRM Wing Model

Pekka Koivisto

Preliminary Cold Soaked Fuel Frost Studies with CRM Wing Model

Pekka Koivisto, Arteform Oy

Finnish Transport Safety Agency (Trafi)
Liikenteen turvallisuusvirasto (Trafi)
Trafiksäkerhetsverket (Trafi)
Helsinki Helsingfors 2016

ISBN 978-952-311-165-3
ISSN 2342-0294

FOREWORD

This research report is focused on the characteristics of Cold Soaked Fuel Frost, which is an important subject in aviation safety. It forms part of the studies in the Frostwing project jointly funded by the Finnish Transport Safety Agency, Trafi and United States Federal Aviation Administration, FAA.

The research was performed by the team of Arteform Oy, headed by MSc Juha Kivekäs.

Helsinki, November 15th 2016

Erkki Soinne

Chief Adviser, Aeronautics

Finnish Transport Safety Agency,

Index

ABSTRACT

Nomenclature

1 Introduction	1
2 Objectives.....	1
3 Test Arrangements	2
3.1 Wind Tunnel	2
3.2 Wing Section Model	2
4 Data Acquisition	3
5 The Simulation of CSFF	4
6 Measurement Program	4
6.1 Lift Degradation as a Take-off Performance Criterion	4
6.2 Wing Section Configuration and Take-off Sequence	6
7 Test Results	7
7.1 General Qualitative Observations	7
7.2 Lift Degradation after Rotation.....	8
8 Conclusions	10
References	11

ABSTRACT

Effects of Cold Soaked Fuel Frost on wing section lift degradation were studied in Aalto University Low Speed Wind Tunnel during September 2016. Cold Soaked Fuel Frost (CSFF) is a frost created only on the wing fuel tank area during an airliner turnaround time due to the fuel that is considerably colder than the surrounding air. The wind tunnel model used in the study was a three element two dimensional CRM (Common Research Model) wing section with a chord of 0.63 m. The wind tunnel test section is 2 m x 2 m. The tests conducted consisted of take-off simulations with an approximately linear acceleration up to the speed of 60 m/s (120 kt) followed by a rotation to a predetermined angle of attack for an additional 50 s. The frost on the fuel tank area was real frost not a simulated equivalent sand paper roughness. Two different average frost thicknesses $k = 0.25$ mm ($k/c = 0.04$ %) to $k = 1,39$ mm ($k/c = 0.22$ %) were generated for the tests. A time dependency of the frost effects due to frost sublimation and melting in air stream was detected which showed the transiency of the lift degradation. The air temperature (OAT) during the tests was 8°C. The fuel tank temperature was -18°C.

Nomenclature

AAT	Aerodynamic Acceptance Test
c	Wing chord
C_L	Lift coefficient
CSFF	Cold Soaked Fuel Frost, frost on wing surfaces at wing fuel tank area generated by cold fuel
k	Frost thickness
OAT	Outside air temperature – here also Wind Tunnel Air Temperature
x/c	Chordwise relative coordinate
V_1	Decision speed
V_{1sr}	Reference stall speed
V_R	Rotation speed
V_2	Take-off safety speed
α	Angle of attack

1 Introduction

There is a clear difference between the operative regulations of US and Europe considering the frost related wing contamination restrictions on take-off. The US regulation (14 CFR 121.629(b)) is undisputed on deposits of frost whereas the European regulation (EU-OPS 1.345 (b)) allows a contamination, provided it does not have any adverse effect on the aircraft aerodynamic performance or controllability. The regulatory differences are described in more detail in Chapter 6.1. This window of opportunity of non-US regulations – especially European and Canadian regulations - has been utilized by Boeing. The Boeing 737 NG model is authorized for limited Cold Soaked Fuel Frost¹ on wing upper surface at take-off as defined in the AFM (Aircraft Flight Manual).

There is a lot of published studies of contamination effects on wing aerodynamics. Part of these studies are addressing the problem of frost^{2,3}. Generally, however these studies concentrate on situations where the wing upper side is covered with an artificial roughness (sand paper or other) along the whole chord. Most of the studies on frost effects consider the so called Hoar (radiation) Frost utilizing plastic or other artificial grain simulation of the real frost texture. To address profoundly the effects of CSFF the aerodynamic deterioration of a wing should be studied with a real Cold Soaked Fuel Frost located on the applicable area of wing upper surface. The present study is the second public one⁴ on CSFF where the frost examined is actual cold soaked frost.

The present study is based on wind tunnel tests at Arteform Low Speed Wind Tunnel carried out during September 2016 utilizing a rotational 3 element 2 dimensional wing section model. The wing section geometry has been chosen as a section cut from the NASA Common Research Model⁵ wing.

It is reasonable to compare the aerodynamic degradation caused by CSFF with the corresponding degradation caused by anti/de-icing fluids as these two are the alternatives in real life: either depart with CSFF or de-ice/anti-ice the wing before the departure.

As the so called Aerodynamic Acceptance Test (AAT) forms the reference for analyzing the aerodynamic effects of the de/anti-icing fluids the present study applies the methodology adopted in wind tunnel tests performed to compose the SAE AS 5900⁶. This means simulated take-off runs in a wind tunnel with accelerating airspeeds up to a typical airliner rotation speed, and then rotating the wing model to an angle of attack representing a lift coefficient typical in a One Engine Out situation at the speed of V_2 . The aerodynamic degradation is determined by comparing the measured lift forces of contaminated and clean wing.

2 Objectives

The objective of this study was to evaluate the effects of CSFF on lift degradation of an airliner wing during a simulated take-off. The parameters affecting the frost effects in the tests are the initial mean thickness and the structure of the frost layer and the Outside Air Temperature (OAT) which in the wind tunnel tests equals to the test section temperature. The effects of these parameters will be studied during the late autumn 2016 and early spring 2017 however the present paper is an initial evaluation of the test arrangements and the new model. In this study only two different thicknesses of frost were created and tested. The results with these two different frost thicknesses will also be compared with the earlier tests⁴ in the same wind tunnel done for a different wing section (DLR-F15).

3 Test Arrangements

3.1 Wind Tunnel

Arteform Low Speed Wind Tunnel is a closed circuit wind tunnel with an octagonal test section with dimensions of 2 m x 2 m and a test section length of 4 m. The flow uniformity in the test section is $< 0.14\%$, and turbulence level $< 0.28\%$ at the wind tunnel speed of 60 m/s. The massive concrete structures of the wind tunnel ducts are outside the facility building. This makes the tunnel structure during winter time an efficient heat sink and the fan power dissipated during short period take-off run simulation does not increase the test section temperature significantly ($< 2^\circ\text{C}$). Temperatures in the test section follow roughly the daily outside air temperature (OAT). During the tests of this study the wind tunnel air temperature was approximately 8°C .

3.2 Wing Section Model

All tests of the present study were conducted with a two dimensional 3 element rotating model that was mounted to a three component balance to measure the aerodynamic lift, drag and pitching moment. The wing section geometry was selected from the CRM wing⁵. The selection criteria are described in detail in reference 7. The model chord was 0.63 m and span 1.55 m which implies an area of 0.969 m^2 . Figure 1 illustrates the wing section geometry and its parts (slat and flap).

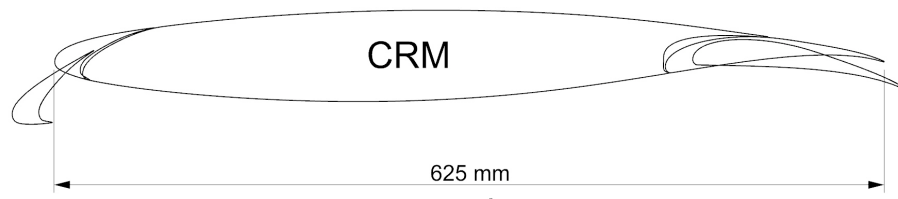


Figure 1. The geometry of the selected wing section⁷ and its parts (slat and flaps)

The load carrying structure of the wing model is mainly made of aerospace aluminum alloys. Bonding of parts are accomplished using epoxy adhesives. The skin thickness on the "Fuel Tank" area is 1,5mm. The skin material is aerospace aluminum alloy. The slats and flaps are made of carbon fiber. The model was equipped with end plates to reduce the three dimensionality of the flow. Two dimensionality and absence of flow separations were confirmed by tufts.

The wing model was equipped with a glycol coolant tank of approximately 27 kg of 50/50 glycol water mixture to simulate the effect of cold fuel in a wing tank. The tank was cooled down using a cooling circuit including a heat exchanger inside the tank - Fig 2. The circuit consisted of a cooling machine outside of the test section and tubes through the test section wall into the tank (Fig. 3). Figure 3 illustrates also the size and shape of the wing model endplates. The coolant tank temperature was monitored via several temperature sensors inside the coolant tank.

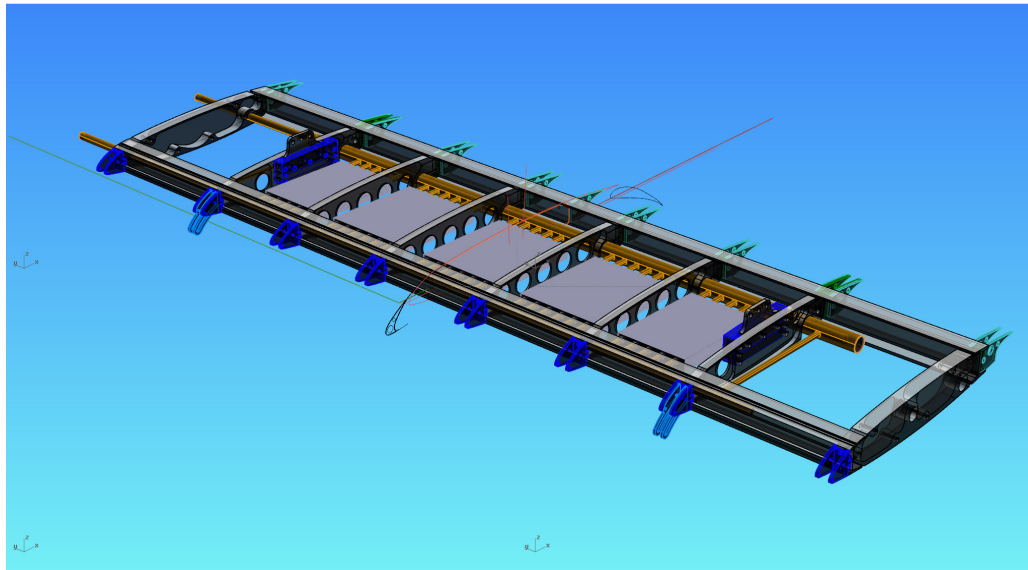


Figure 2. Coolant circuit inside the "Fuel Tank". Heat exchanger and its tubes visible between the second and seventh ribs.

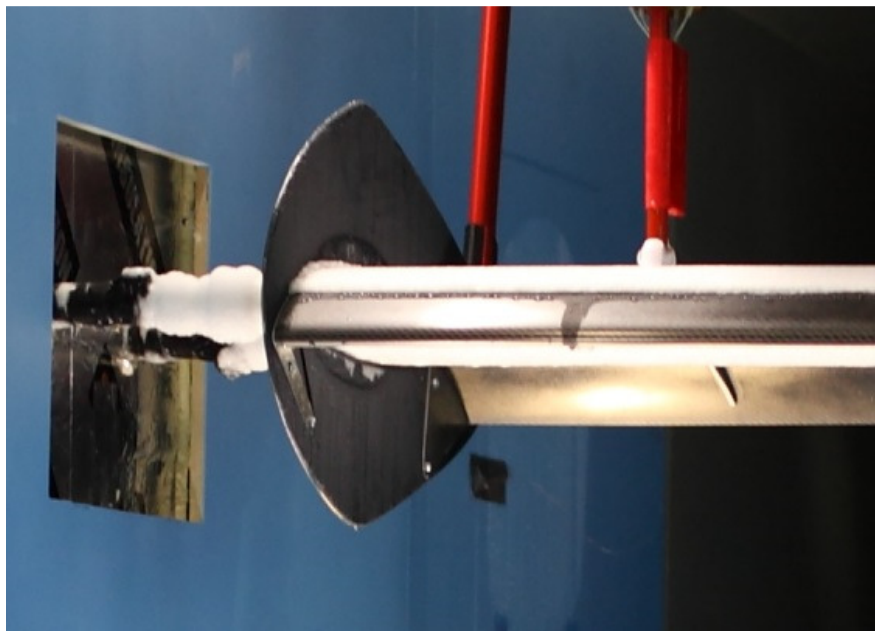


Figure 3. The coolant tank interface in the test section

The wing model coolant tank which simulates an airliner fuel tank is positioned between the relative chord coordinates of $x/c = 12\%$ and 65% . The area of the fuel tank is therefore 53% of the reference wing area.

4 Data Acquisition

There is a standard measuring software in the wind tunnel collecting the wind tunnel temperature, airspeed, dynamic pressure, relative humidity, balance forces and moments (lift, drag and pitching moment) and the wing angle of attack.

The temperature of the coolant tank was measured separately to follow the coolant mean temperature during each test. The coolant temperature was not controlled during the tests as the tubes from the tank to the cooling machine were disconnected for the test periods. There were 10 temperature sensors in fuel tank inner skin, outer skin and within the fuel.

The effect of frost on the wing tank area on the take-off performance is evaluated by measuring the lift coefficient degradation ΔC_L due to the CSFF contamination. This means sequential C_L measurements of the clean wing and a contaminated wing. As the result is a difference between the two lift coefficients at the same angle of attack the repeatability of the tests is more relevant than the absolute accuracy of the lift coefficient itself. However, in this preliminary stage there were only two pair (clean vs. frost) of tests done and it is not statistically meaningful to define any repeatability based on these tests. The two clean wing lift coefficients were 1,505 and 1,549 which means a "repeatability" of 0,006 or 0,4 %.

5 The Simulation of CSFF

To get the wing model coolant tank area frosted the cooling circuit is operated several hours or even overnight. The test section was initially designed to be locally cooled down to achieve different ambient temperatures. However, it appeared that the conditioning of air dried it up with the result of very thin frost layers. Due to this the cooling of test section was abandoned and the natural ambient temperature was accepted to be a non-controllable parameter.

The created frost thickness was measured with an Elcometer thickness gauge from 9 evenly spaced points in the tank area on the upper surface of the wing. The frost densities or liquid water contents were not measured in this study. One of the objectives of the project is to measure later on the frost and its structure using laser-scanning.

The average thickness values during the two tests were 1,39 mm with a standard deviation of 0,18 mm and 0,25 mm with a standard deviation of 0,05mm. The corresponding relative roughness values (k/c) are $2,2 \cdot 10^{-3}$ and $0,4 \cdot 10^{-3}$.

6 Measurement Program

6.1 Lift Degradation as a Take-off Performance Criterion

The objective of a take-off simulation wind tunnel test is to simulate the One Engine Inoperative (OEI) situation where the airliner is flying at the speed of V_2 after lift-off up to the so called "cleaning altitude" at which the flaps and slats are retracted (>400 ft above ground level as per EASA CS 25.121⁸ see figure 4).

The effects of frost contamination (EASA and Transport Canada Certification Standards) or de/anti-icing fluid application (all Certification Standards including the US FAR 25) to the take-off performance of an airliner have not been addressed in the certification standards. However, a "non-written" policy exists that

addresses these contaminants with the requirements considering the inflight icing.

The requirement applied for the frost and de/anti-icing fluid contaminant (common for EASA, TC and FAA) is as follows:

"25.121 (b)(2) Climb one engine inoperative, Take-off; landing gear retracted: The requirements of subparagraph (b)(1) of this paragraph must be met:

(i) In non-icing conditions; and

(ii) In icing conditions with the "Take-off Ice" accretion defined in Appendix C, if in the configuration of CS 25.121(b) with the "Take-off Ice" accretion:

(A) The stall speed at maximum take-off weight exceeds that in non-icing conditions by more than the greater of 5.6 km/h (3 knots) CAS or 3% of VSR; or

(B) The degradation of the gradient of climb determined in accordance with CS 25.121(b) is greater than one-half of the applicable actual-to-net take-off flight path gradient reduction defined in CS 25.115(b)"

This means that if V_{SR} in the configuration defined by CS 25.121(b) with the "Takeoff Ice" accretion defined in Appendix C to CS-25 exceeds V_{SR} for the same configuration without ice accretion by more than the greater of 3 knots or 3% or the degradation of the gradient of climb is greater than 0.4 % for 2-engine aircraft, the take-off demonstrations should be repeated to substantiate the speed schedule and distances for take-off in icing conditions. In case of CSFF this requirement is applied as such for frost contamination. In case of de/anti-icing fluids Hill and Zierter⁹ evaluated several specific take-off performance criteria following FAR 25 while developing the Aerodynamic Acceptance Test for fluids and ended up to select the stall speed part of the above regulation (25.121 (b)(2)(A)) as the critical one.

If frost is considered to remain on the wing considerably above the cleaning altitude (400 ft AGL) it is obvious that there is a possibility that the climb gradient will be more critical than the lift stall speed degradation. However, in a wind tunnel test for a wing model the only relevant restriction to be studied is naturally the stall speed restriction.

The stall speed margin degradation of 3% may be interpreted as a lift coefficient (C_L) degradation of 5.24 % at the selected "lift off" angle of attack. For a detailed reasoning of this see Ref 10.

Regarding both de/anti-icing fluid tests and frost tests in wind tunnel the negative temperature gradient during initial climb will not be taken into account. As the standard atmosphere temperature gradient is approximately only 2°C/1000ft this is not considered in the analysis presented here.

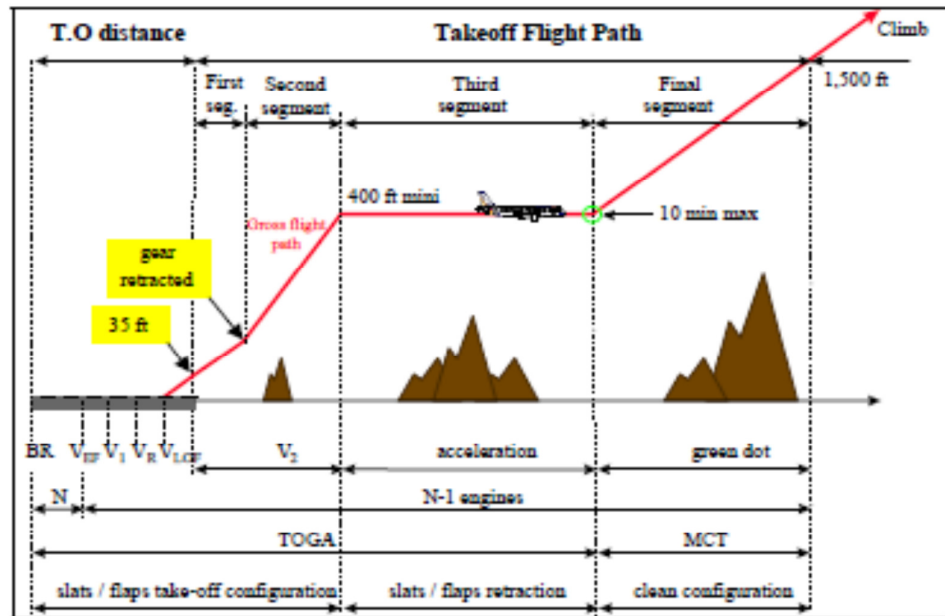


Figure 4. Take-off flight path as per EASA CS 25.12.

6.2 Wing Section Configuration and Take-off Sequence

A take-off sequence (engine failure at speed V_1) of an airliner consists of (see Fig. 4.):

- Acceleration from stand still to the rotation speed (V_R) with a constant pitch attitude during ground roll
- After reaching V_R the pitch attitude is increased to a lift off attitude (normally a predetermined constant value e.g. 15°)
- Once airborne the airspeed is accelerated to V_2 where it remains until reaching the cleaning altitude at which the slats and flaps are retracted

To simulate in a wind tunnel the speed sequence in detail, as given above is too complicated a task. A generally adopted simplification among the AAT –research tests documented¹⁰ is to accelerate the speed from wind tunnel idle speed as linearly as possible to V_2 and then rotate the wing section to a predetermined angle of attack and keep it there for a predetermined time – e.g. 30 s.

For a real airliner wing lift coefficient history simulation at take-off there should be approximately a difference of $\Delta C_L = 0.7 - 0.8$ in C_L between ground roll and initial climb at V_2 (see Ref. 11 for detailed analysis). The CRM wing section model was tested with several different slat and flap configurations to find a satisfactory combination of angle of attack and lift coefficient both during ground roll and at speed V_2 , which in this case was limited by the maximum wind tunnel speed of 60 m/s (120 kt). After a set of tests, the best configuration appeared to be slats deflected 22° , and flaps 10° which gave the following combinations of angle of attack and lift coefficient:

- Ground roll (acceleration to 60 m/s) $\alpha = 0,0^\circ$ and $C_L = 0,52$
- Speed 60 m/s (V_2) wing section rotated $\alpha = 9,2^\circ$ and $C_L = 1.50$

The chosen speed-angle of attack (α) - time sequence was as follows :

- At $\alpha = 0^\circ$ wind tunnel speed is accelerated from idle speed to 60 m/s.

- As soon as the speed has reached 60 m/s it is kept constant and the wing section is rotated at a rate of $4,5^\circ/s$ to $\alpha = 9,2^\circ$
- After $\alpha = 9,2^\circ$ has been reached the wind tunnel speed is kept at 60 m/s for 60 seconds

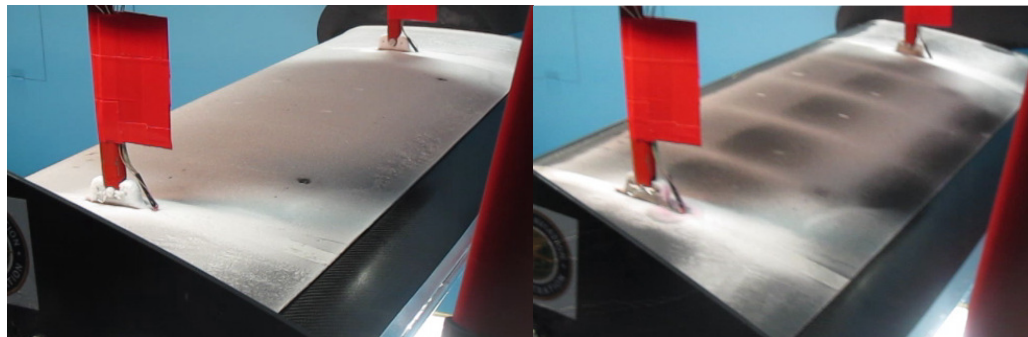
The time used to accelerate the wind tunnel speed to 60 m/s is constant 30 s.

7 Test Results

7.1 General Qualitative Observations

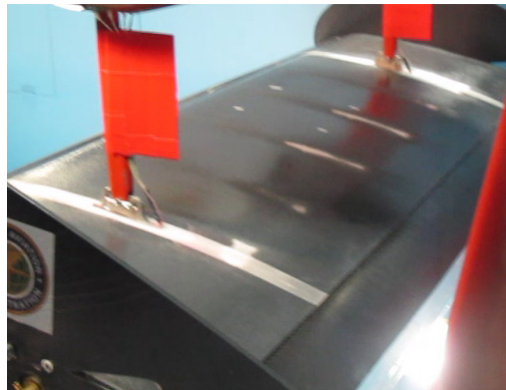
The progress of frost sublimation and/or melting during the test was visualized by a video camera. The changes in the frost layer during the tests are illustrated in Fig. 5. and 6. Though the coolant tank situated chord wise between $x/c = 12\%$ and 65% there appeared frost ahead and behind the foremost and rearmost line of the coolant tank.

According to visual observations the frosted area reduction started from the leading edge area just behind the upper slat opening. There was obviously melting present at the leading edge area as the water ran in liquid form over the upper side. This water however partly turned into clear ice just after the slat opening before the tank area. There may be a separation bubble which contributes the icing. The ice formation was approximately 0,5 mm thick and 10mm long (chordwise). This clear ice formation separated and flew off the surface after approximately 60 seconds after the rotation.



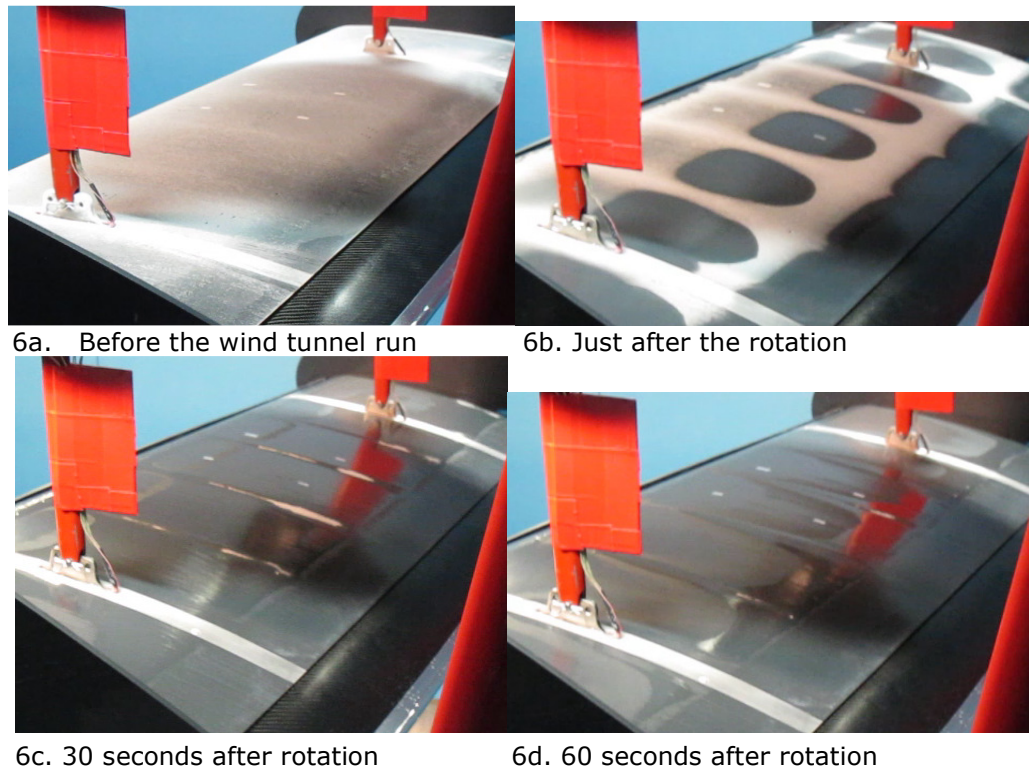
5a. Before the wind tunnel run

5b. Just after rotation



5c. 30 seconds after rotation

Figure 5. 1,39 mm thick frost ($1000 \cdot k/c = 2,2$) on the upper side of the wing model. OAT = 8°C and "fuel" temperature = -18°C .



6a. Before the wind tunnel run

6b. Just after the rotation

6c. 30 seconds after rotation

6d. 60 seconds after rotation

Figure 6. 0,25 mm ($1000 \cdot k/c=0,4$) thick frost on the upper side of the wing model. OAT = 8°C and "fuel" temperature = -18°C.

7.2 Lift Degradation after Rotation

To determine the lift degradation, the clean wing case was measured after both frost tests to eliminate daily changing factors on the results. In the following the lift degradation variation in time is presented in figures where time point 0 represents the situation where rotation has just ended and angle of attack $\alpha = 9,2^\circ$ has been reached. Results are presented in per cents (%) of clean wing lift coefficient. As reasoned above in chapter 6.1 an acceptable lift coefficient loss may be considered as 5.24 %.

The results of lift coefficient degradation tests are illustrated in Figures 7 and 8. Figure 7 shows the test results for 1,39mm frost and Figure 8 for 0,25mm frost.

In both cases the wind tunnel air temperature (OAT) was 8°C and the wing tank ("fuel tank") temperature -18°C. In both cases there is a gradual decrease of lift degradation which first settles to a fairly constant value for a period of 10-20 seconds. This is followed by an abrupt drop to zero within a few seconds. The timing of this clear drop of lift degradation is well in line with visual observations of the clear ice separation from the leading edge area described in section 7.1.

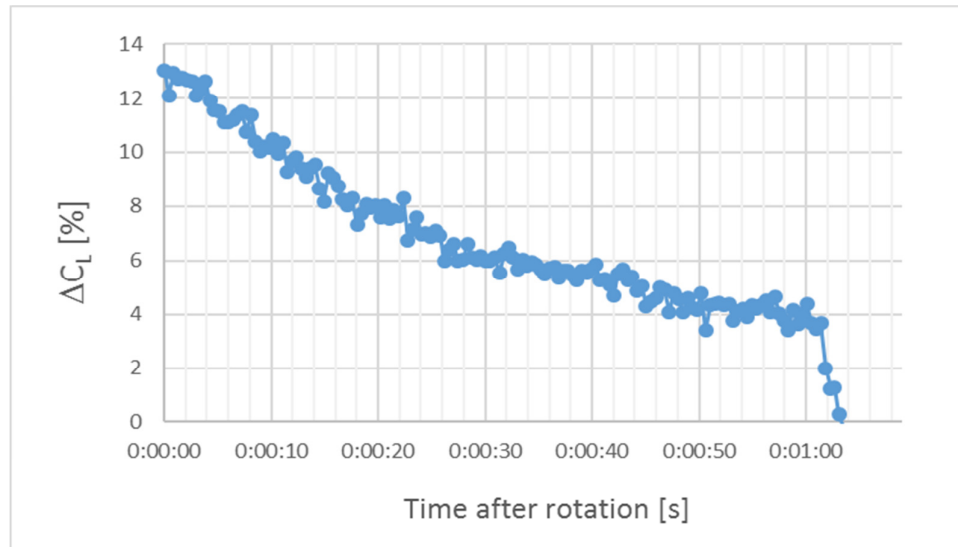


Figure 7. CRM wing model lift coefficient degradation variation with time after rotation for 1,39mm ($1000 * k/c = 2,2$) frost thickness

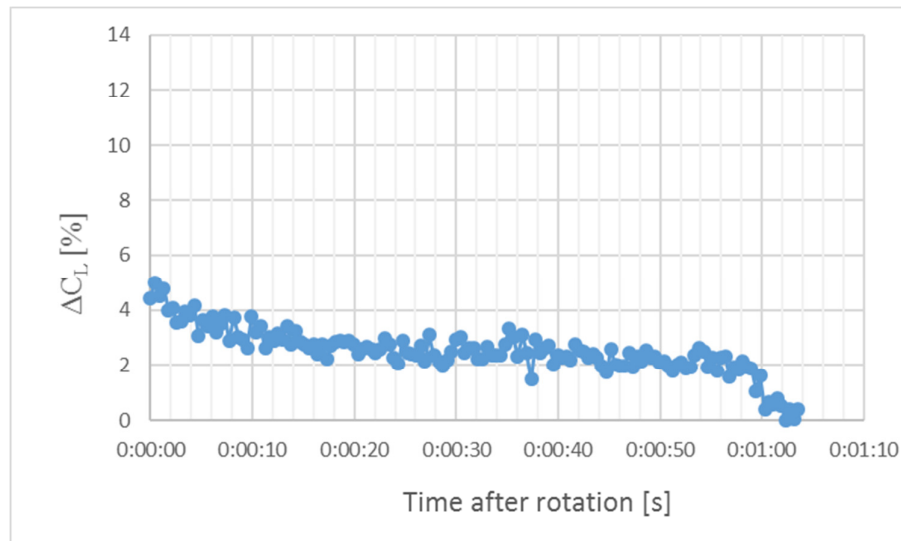


Figure 8. CRM wing model lift coefficient degradation variation with time after rotation for 0,25mm ($1000 * k/c = 0,4$) frost thickness

Some results of a previously published study for DLR-F15 profile⁴ with two different frost thicknesses are illustrated in Fig. 9. The frost thickness of Fig. 8. is between the values of Fig 9. There is a 3°C difference in OAT-values of Fig. 8 and 9. both being clearly above the freezing point. The lift degradation initial value and the value at 30 seconds after rotation are fairly close each other. The chord of DLR- F15 model was 0,65m which is only 3% more than the chord of present study CRM model. Unfortunately, the final value of lift degradation after 60 seconds were never measured as the wind tunnel run ended to 40 seconds after rotation. However, there was no similar clear ice buildup visible in the case of DLR-F15 tests.

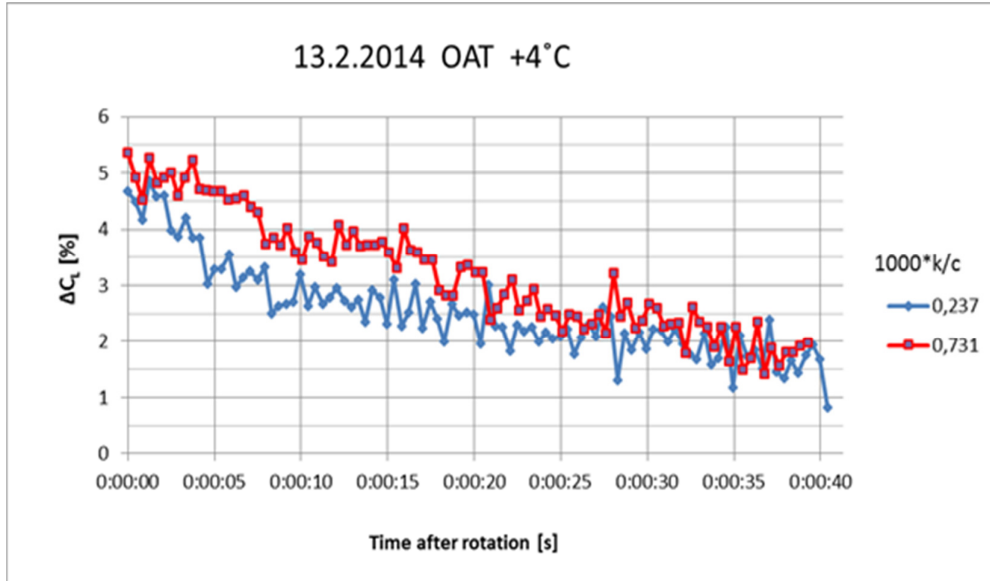


Figure 9. DLR- F15 wing model lift coefficient degradation variation with time after rotation for 0,15 mm ($1000 \cdot k/c = 0,237$) and 0,48 mm ($1000 \cdot k/c = 0,731$) frost thickness⁴.

8 Conclusions

Wind tunnel experiments for a NASA -CRM three element wing section model were conducted at Arteform Low Speed Wind Tunnel facility during October 2016. The objectives of the study were to evaluate the functionality of the test arrangements and to compare the initial results with previous results received from previous tests.

The tests were done with two different frost layers and one ambient temperature of 8°C. The results showed the transient nature of lift degradation during the test run which resembled the results of the previous study. However, a clear distinction from the previous study was the formation of clear ice on the leading edge area resulting probably to an additional lift degradation which disappeared at the point when the ice separated from the wing model surface.

References

1. Adrian, P., Brightwell J.: "Operating Boeing 737-NG with Cold – Soaked Fuel Frost", Presentation given at EASA Annual Safety Conference at Cologne, Germany, 15-16th October 2013.
2. Ljungström, B.L.G.: "Windtunnel investigation of simulated hoar frost on a two-dimensional wing section with and without high lift devices." Report FFA-AU-902, April 1972
3. Kind, R.J., Lawrysyn, M.A.: "Performance Degradation due to Hoar Frost on Lifting Surfaces." Canadian Aeronautics and Space Journal, Vol 38, No. 2, June 1992.
4. Koivisto, P.: "Effects of Cold Soaked Fuel Frost on Lift Degradation during Simulated Take-off", Trafi Reports 4-2015, September 2015
5. Lacy, D.S. and Sclafani, A.J. "Development of the High Lift Common Research Model (HL-CRM): A Representative High Lift Configuration for Transonic Transports", AIAA 2016-0308, 54th AIAA Aerospace Sciences Meeting, 4-8 January 2016, San Diego, California, USA
6. "Standard Test Method for Aerodynamic Acceptance of SAE AMS 1424 and SAE AMS 1428 Aircraft Deicing/ Anti-icing Fluids", AS5900 Rev.B , SAE International, 26 July 2007.
7. Kivekäs, J. "NASA HL-CRM (take-off) 2D-section definition for Frostwing-studies", Arteform Ltd Memo 20160430, April 2016.
8. Certification Specifications and Acceptable Means of Compliance for Large Aeroplanes, CS-25 Amendment 13, 10 June 2013, Annex to ED Decision 2013/010/R, Amendment
9. Hill, E.G., and Zierten, T.A., "Aerodynamic Effects of Aircraft Ground Deicing /Anti - Icing Fluids," Journal of Aircraft, V o l. 3 0, N o. 1 , Jan. -Feb., 1993
10. Broeren, A., Riley, J: "Review of the Aerodynamic Acceptance Test and Application to Anti-icing Fluids Testing in the NRC Propulsion and Icing Wind Tunnel" NASA TM 2012-216014, Aug. 2012.
11. Koivisto, P. "Effects of Ant-icing Treatment on Lift Degradation during Simulated Take-off", Trafi Publications 25/2013.